Editors' Suggestion | Featured in Physics

Optically Controlled Femtosecond Polariton Switch at Room Temperature

Fei Chen,[1] Hui Li,[1,*] Hang Zhou,[2] Song Luo,[2] Zheng Sun,[1] Ziyu Ye,[1] Fenghao Sun,[1] Jiawei Wang,[1] Yuanlin Zheng,[3] Xianfeng Chen,[3,4] Huailiang Xu,[1] Hongxing Xu,[1] Tim Byrnes,[5,1,6,7,8,†] Zhanghai Chen,[2,11,12,‡] and Jian Wu[1,6,9,10,§]

[1]*State Key Laboratory of Precision Spectroscopy, East China Normal University, Shanghai 200241, China*
[2]*Department of Physics, College of Physical Science and Technology, Xiamen University, Xiamen 361005, China*
[3]*State Key Laboratory of Advanced Optical Communication Systems and Networks, School of Physics and Astronomy, Shanghai Jiao Tong University, Shanghai 200240, China*
[4]*Collaborative Innovation Center of Light Manipulation and Applications, Shandong Normal University, Jinan 250358, China*
[5]*Division of Arts and Sciences, New York University Shanghai, 1555 Century Ave, Pudong New District, Shanghai 200122, China*
[6]*NYU-ECNU Institute of Physics at NYU Shanghai, 3663 Zhongshan Road North, Shanghai 200062, China*
[7]*Center for Quantum and Topological Systems (CQTS), NYUAD Research Institute, New York University Abu Dhabi, UAE*
[8]*Department of Physics, New York University, New York, New York 10003, USA*
[9]*Collaborative Innovation Center of Extreme Optics, Shanxi University, Taiyuan, Shanxi 030006, China*
[10]*CAS Center for Excellence in Ultra-intense Laser Science, Shanghai 201800, China*
[11]*Wuhan National High Magnetic Field Center, Wuhan 430074, China*
[12]*Collaborative Innovation Center of Advanced Microstructures, Nanjing University, Nanjing, Jiangsu 210093, China*

(Received 15 December 2021; revised 4 April 2022; accepted 17 June 2022; published 29 July 2022)

Exciton polaritons have shown great potential for applications such as low-threshold lasing, quantum simulation, and dissipation-free circuits. In this paper, we realize a room temperature ultrafast polaritonic switch where the Bose-Einstein condensate population can be depleted at the hundred femtosecond timescale with high extinction ratios. This is achieved by applying an ultrashort optical control pulse, inducing parametric scattering within the photon part of the polariton condensate via a four-wave mixing process. Using a femtosecond angle-resolved spectroscopic imaging technique, the erasure and revival of the polariton condensates can be visualized. The condensate depletion and revival are well modeled by an open-dissipative Gross-Pitaevskii equation including parametric scattering process. This pushes the speed frontier of all-optical controlled polaritonic switches at room temperature towards the THz regime.

DOI: 10.1103/PhysRevLett.129.057402

Optical and optoelectronic devices have been investigated in the context of numerous information processing applications, with the aim of enabling high operation speeds [1,2]. A core component of such devices are switches which are based on nonlinear optical effects and have been investigated in several works [3–5]. The performance of such devices is typically limited by the strength of the optical nonlinearity, and can be enhanced using artificial photonic structures [6]. Taking advantage of the highly nonlinear interactions between ultrashort optical pulses in dielectrics, it was shown that electric currents can be steered on sub-femtosecond timescales, promising signal processing at the PHz (10^{15} Hz) regime [7]. However, this technique requires high complexity both in terms of the fabrication of sub-wavelength structures, and for the high-resolution light-field manipulations at the attosecond scale, since electron dynamics are sensitive to the subcycle evolution of the optical field. Moreover, the ultrafast movement of carrier charges induced by the waveform controlled light field is challenging in terms of cascadability and integration. In this sense, alternative methods for ultrafast switches are of interest towards real-life applications.

Meanwhile, rapid progress has been made recently with exciton polaritons, which are hybrid quasiparticles of matter and light, and thus are potentially highly applicable to optoelectronics. Exciton polaritons are formed due to the strong coupling between microcavity photons and excitons, with properties inherited from their constituent particles [8,9]. On the one hand, its photonic nature results in a very light effective mass [10]. This allows for polaritons to undergo Bose-Einstein condensation (BEC) at high temperatures [10,11] many orders of magnitude higher than for an atomic BEC, which usually occurs at nanokelvins [12]. Phenomena such as superfluidity [13], vortex [14], soliton formation [15,16], and the realization of novel states of matter [17,18] have been experimentally observed, which typically are performed at cryogenic temperatures (e.g., for GaAs or CdSe). However, for practical applications it is much more desirable to manipulate the polariton wave packets at room temperature. For this, alternative materials with higher exciton binding energies are required such that ambient temperatures (with thermal energy around 26 meV) do not disassociate the excitons. In semiconductor microcavities with gain mediums such as ZnO, the group III-nitrides, and certain perovskites, BEC of polaritons is

realizable at room temperature [19–21], making them promising candidates for practical devices. Additionally, polaritons have strong nonlinear properties that originate from the Coulomb exchange interaction of their excitonic parts [22]. This nonlinearity can be taken advantage of for the purposes of tailoring the polaritons to applications in optoelectronics.

Several applications of polaritons towards optoelectronics have been experimentally demonstrated. A polariton light-emitting diode [23] and polariton lasing at power thresholds orders of magnitude lower than in standard optical lasers [24] have been realized. Polariton fluids moving in tailored microcavities were used to demonstrate an all-optical transistor. AND/OR logical gates were demonstrated in GaAs/AlAs and organic semiconductor microcavities [25,26]. Polariton switches with an operational speed in the picosecond regime were reported based on light-induced manipulation of the energy landscapes [27,28]. A spin-switch based on optical trapping of polariton condensates was realized for ultralow control energies [29]. Recently, single-photon based optical switching and amplification were realized with exciton-polaritons [30].

In this paper, we demonstrate a highly controllable femtosecond polariton switch at room temperature in a one-dimensional (1D) ZnO whispering gallery microcavity. Initially, a polariton condensate is formed by nonresonant pumping (Fig. 1). The population of the polariton condensate can then be controlled by sending another optical pulse at a frequency differing from the pumping pulse, which depletes the polariton condensate at subpicosecond timescales. We show that the ultrafast switching dynamics can be well manipulated by the controlling pulse, supporting THz operational speed and high extinction ratio at room temperature. The dynamics of the subpicosecond switching of polariton condensates are characterized by a femtosecond angle-resolved spectroscopic imaging technique [31–33]. We explain the phenomenon by parametric scattering of the photonic part of the polariton condensate through a four-wave mixing process [34,35].

In our experiment, two ultrashort laser pulses at two different wavelengths were utilized to generate the polariton condensate (the pump pulse) and control the condensate (the control pulse). As shown in Fig. 1(a), a regular hexagonal cross section ZnO microwire with smooth facets forms a high-quality whispering gallery microcavity with radius of ~1.8 μm. The spot size was ~4 μm for the pump beam, and ~16 μm for the control beam. Figure 1(b) shows the schematic energy-momentum dispersion of polaritons in our experiment. A femtosecond pump pulse with a central wavelength of 350 nm (with photon energy higher than the ZnO band gap) excites a large population of high-energy excitons. These hot excitons relax to form an exciton reservoir, from which the polariton condensate forms. Because of the hexagonal microcavity supporting several whispering gallery modes, several lower polariton (LP) branches are present, each with different energies. The polariton lifetime is in the regime of picoseconds. The polaritonic condensation dynamics are explored with femtosecond time resolution as in our previous work, using photoluminescent (PL) emission spectroscopy in the Fourier plane [31,32].

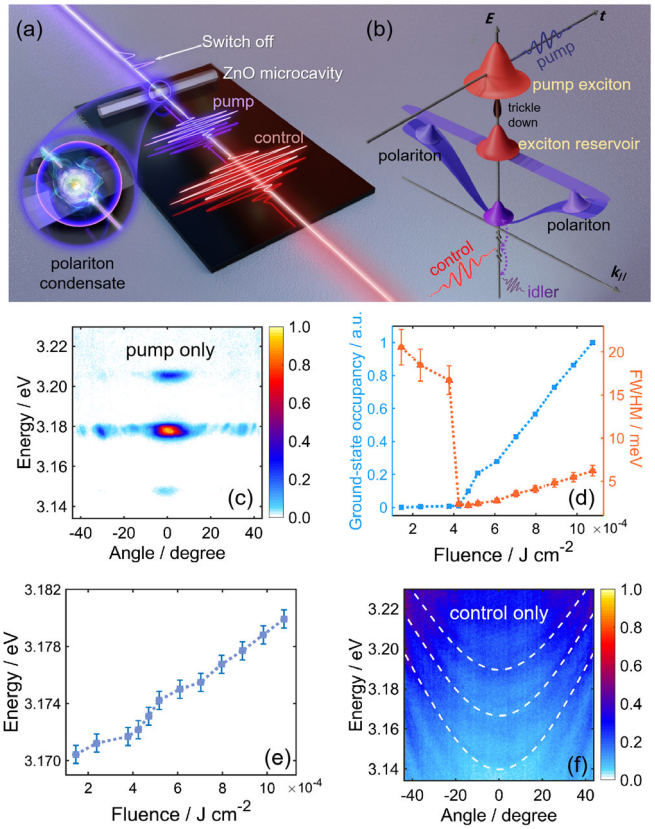

FIG. 1. (a) The experimental scheme. (b) Schematic energy-momentum dispersion for the ZnO microwire. Two photons from the 700 nm control pulse induce stimulated scattering from the polariton condensate formed at around $k_{//} = 0$ on the LP branch. The idler photon is at a long wavelength of 3.4 μm. (c) The integrated angle-resolved PL spectrum obtained at 350 nm at the pump fluence of about 7.0×10^{-4} J/cm^2. The pump fluence dependence of (d) the ground-state occupation, the emission linewidth, and (e) the energy at the maximum of the PL emission spectra. (f) The integrated angle-resolved PL spectrum obtained for excitation at 700 nm at the fluence of 3.4×10^{-3} J/cm^2.

Figure 1(c) shows the momentum-resolved PL emission when the ZnO microwire is illuminated by the 350 nm pump pulse with fluence ~7.0×10^{-4} J/cm^2, without application of the control pulse. The PL emission shows condensation behavior close to $k_{//} = 0$. Figures 1(d) and 1(e) show the pump fluence dependence of the ground-state occupation, the corresponding linewidth (noted as full-width at half-maximum, FWHM), and the photon energy at the maximum of the PL emission spectrum. For a pump fluence exceeding the condensation threshold

of $\sim 4.2 \times 10^{-4}$ J/cm^2, we can see the dramatic increase of the ground state population and a collapse of the linewidth, accompanying an energy blueshift. These indicate the formation of a polariton condensate in the strong coupling regime [10,36–39]. With a pump power of $6P_{\mathrm{th}}$, polariton condensates are formed on multiple LP branches [Fig. 2(a)], involving rich dynamics as was investigated in our previous work [31]. Femtosecond polariton lasing on individual LP branches can be clearly observed. Figure 1(f) shows the dispersion image of the control pulse alone, without the pump pulse. The control pulses at 700 nm were guided through a precisely controlled delay stage and finally propagated collinearly with the pump pulses towards the microcavity. We observe that LPs can be excited in the ZnO microcavities through a two-photon process. This indicates that ZnO has an appreciable nonlinearity which couples the LP and the 700 nm modes. However, the efficiency of such a process is orders of magnitude lower than by direct excitation with 350 nm photons. Hence for the regime that is examined in this experiment, a polariton condensate cannot be generated by the control beam alone.

In Fig. 2, we show the time-resolved, momentum-integrated PL spectra for the pump and control beams together. Here the pump power is around $6P_{\mathrm{th}}$. The control pulse is fixed to a fluence of about 2.9×10^{-3} J/cm^2 and delayed with respect to the pump pulse by various times. The arrival time of the pump pulse is defined as the zero point on the time axis. As seen in Figs. 2(b)–2(f), the PL emission from multiple LP branches can be efficiently switched off by the control beam for the various delay times as marked. The control pulse duration of $\sim$200 fs is indicated by the gray area. The timing of the turn-off is almost being synchronized for all the LP branches. The switching time, defined as the time that the signal decreases from 90% to 10% of its maximum value is around 390 fs [as seen particularly in Fig. 2(d)], corresponding to an operational speed of about 2.5 THz. Interestingly, condensate revivals were observed long after the control pulse is complete [e.g., after around 4 ps in Fig. 2(c)].

Figure 3 shows the dependence on the control pulse fluence at a fixed pumping power of about $6P_{\mathrm{th}}$. The control pulses arrive at about 2.4 ps for the measurements shown in Figs. 3(b)–3(d). At high control pulse fluences, we observe that a very high extinction ratio can be attained. Taking the data shown in Fig. 3(b) as an example, by setting the appropriate background level in the observed dynamics, we obtain an extinction ratio of above 50 dB. We note that the pump power needed for polariton condensation is relatively low compared to other types of lasers where population inversion is required. The intensities of both the pump and the control beam in our work in absolute terms are still very low, equating to very low energy consumption levels. We observe that the duration of the off-state increases with the control beam fluence. To avoid sample damage, we did not further increase the control beam fluence for the measurements presented in Fig. 3. Nevertheless, systematic control-fluence-dependent measurements of the polaritonic switching dynamics have been performed for a fixed pump power and are shown in Sec. V of the Supplemental Material [40]. A cutting off time within 300 fs can be obtained.

We found that the "off" time of the switch increases almost linearly with increasing control fluence, and the extinction ratio shows a monotonic increasing first and being saturated at around 60 dB. The saturation of the extinction ratio is due to a nearly complete depletion of the polaritonic population through the parametric scattering process.

The switching times as shown in Figs. 2 and 3 and 3 were all in the subpicosecond regime. Similar ultrafast switching behavior was also realized by using an 800 nm femtosecond laser pulses as the control pulses (see the section IV in the Supplemental Material [40] for further details). We

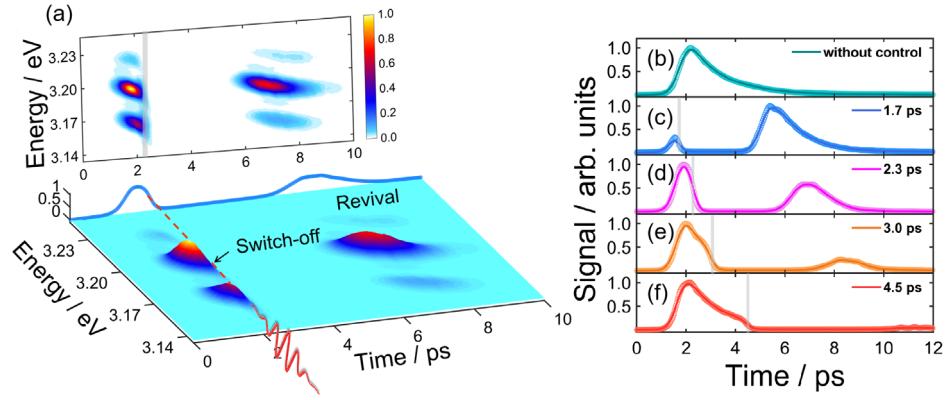

FIG. 2. Control pulse delay dependence of polariton condensate population for fixed control power. The pump power is $\sim 6P_{\mathrm{th}}$. The fluence of the control pulse is about 2.9×10^{-3} J/cm^2. (a) The time-resolved, momentum-integrated PL spectra. The integrated signal from all the LP branches to the time axis with (b) no control pulse, control pulse with delay at (c) 1.7, (d) 2.3, (e) 3.0, and (f) 4.5 ps. The duration and the arrival time of the control pulses are indicated by the gray areas.

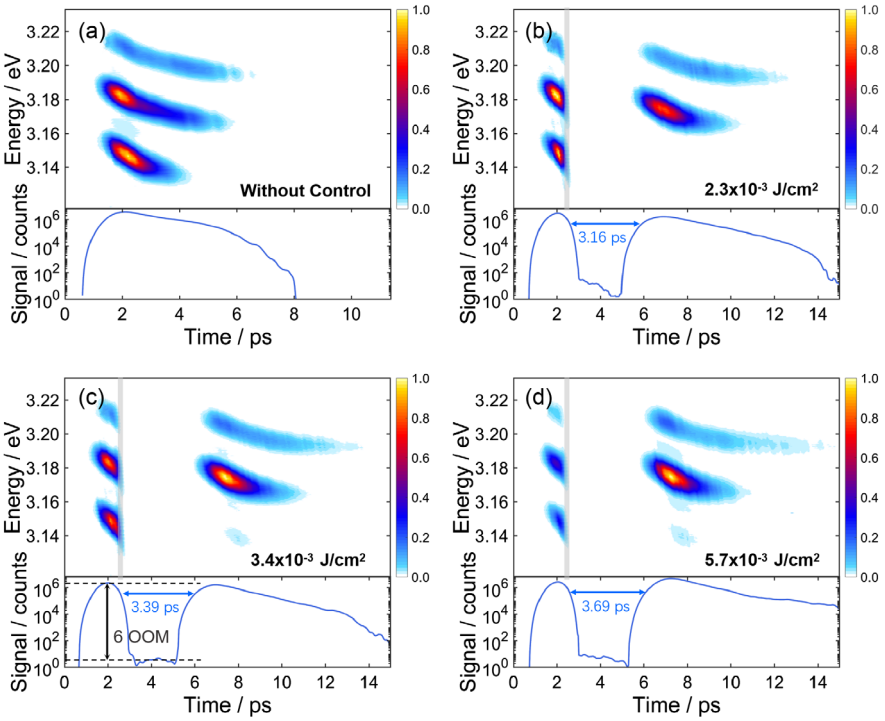

FIG. 3. Control pulse power dependence of polariton condensate population for fixed control pulse delay at 2.4 ps. Color images shown are the time-resolved, momentum-integrated PL spectra. The pump power is $\sim 6P_{\mathrm{th}}$ for all cases with (a) no control pulse, control pulse fluence at (b) 2.3×10^{-3} J/cm^2, (c) 3.4×10^{-3} J/cm^2, (d) 5.7×10^{-3} J/cm^2. The blue curves represent the integrated signal from all the LP branches. The blue arrows indicate the times where the polariton is switched off. The black arrow in (c) indicates the 6 orders of magnitude (OOM) difference between the "on" and the "off" states.

attribute the ultrafast switch-off of the polariton condensate to parametric scattering from the LP modes to the control pulse mode. As shown in Fig. 1(b), ZnO supports a nonlinear process such that two photons from the 700 nm control pulse can be converted to a LP mode with energy ~390 nm. When there are both a large LP and 700 nm photon population, the reverse process of a LP being converted to two 700 nm photons is bosonically enhanced and opens a strong channel for scattering of the LPs. We note that polariton-parametric-scattering-based phenomena producing entangled signal and idler pairs and realization of polariton inversion were reported in a different context [45,46].

To confirm this picture of polariton switching, an open-dissipative Gross-Pitaevskii (GP) equation coupled to an incoherent reservoir and the four-wave mixing modes were used to simulate the dynamics. To model the polariton condensation, we consider the LP mode amplitude ψ to be coupled to an incoherent reservoir density n_R [43,44]. The incoherent reservoir is in turn coupled to a population of high-energy excitons n_P, which is initially excited by the pump laser. Photonic parametric scattering (which is based on a different physical process compared to the polaritonic parametric scattering explored in previous work [31]) is considered to occur between the polariton condensate and the 700 nm control pulse ϕ. To satisfy energy conservation, the parametric scattering requires another photon at an infrared wavelength, according to $h\omega_1 + h\omega_1 = h\omega_2 + h\omega_3$, where $\omega_{1,2,3}$ correspond to the photon frequencies at wavelengths of 700 nm, 390 nm, and 3.4 μm, respectively. This 3.4 μm idler mode amplitude is denoted ξ. The equations governing the dynamics are written as

$$i\frac{d\psi}{dt} = \left[-\frac{i\gamma}{2} + \frac{iR}{2}n_R\right]\psi - i\kappa\phi^{*2}\xi, \tag{1}$$

$$\frac{dn_R}{dt} = rn_P - \gamma_R n_R - Rn_R|\psi|^2, \tag{2}$$

$$\frac{dn_P}{dt} = P(t) - \gamma_R n_P - rn_P, \tag{3}$$

$$\frac{d\phi}{dt} = P_b(t) - \frac{\gamma_b}{2}\varphi - 2\kappa\phi^*\psi^*\xi, \tag{4}$$

$$\frac{d\xi}{dt} = -\frac{\gamma_c}{2}\xi + \kappa\psi\phi^2. \tag{5}$$

Here $P(t)$ is the pump laser power; R is the reservoir-condensate scattering rate; γ, γ_R, γ_b, γ_c are the decay rate of the LPs, the excitons, the 700 nm control pulse and the idler photons, respectively; κ represents the parametric scattering

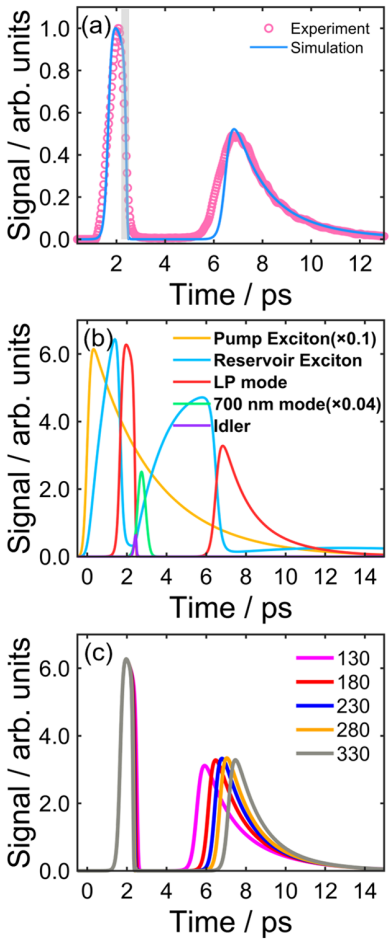

FIG. 4. Numerical simulation of the optical switch using an open-dissipative Gross-Pitaevskii equation. (a) Comparison of the simulated and the experimentally measured polariton signal obtained from the data shown in Fig. 3(b). (b) The calculated dynamics for polariton condensation and the parametric scattering process for the various participating modes as labeled. (c) Effect on polariton revival as a function of control pulse intensity.

rate in the parametric scattering process. Further details of the theoretical model are presented in the Sec. VIII of the Supplemental Material [40].

A comparison of the numerical and experimental results [obtained from the data presented in Fig. 3(b)] is shown in Fig. 4. Excellent agreement between the theory and experiment is obtained. Because of the nearly synchronous turn-off of the polariton branches as seen in Figs. 3 and 4, we consider that this is a reasonable approximation in the context of modeling the polariton switch.

The populations of the pump exciton, the incoherent reservoir, polariton condensate, control pulse, and the idler mode of the calculated dynamics are shown in Fig. 4(b). Initially, the pump excites hot excitons (yellow) which populate the incoherent reservoir (blue). Once there is sufficient population in the reservoir, condensation takes place, and there is a nonlinear gain of the condensate population (red), along with a sharp drop in the reservoir population. When the control beam at 700 nm arrives (green), the polariton signal drops dramatically towards zero, accompanied by the generation of a very weak idler beam (purple). Because of the low intensity and the midinfrared wavelength of the idler, this was out of the range of detection. The long relaxation time of hot excitons allows the exciton reservoir to be repopulated, from which a new polariton condensate can form again when the action of the control pulse has ended. We numerically confirm that by varying the intensity of the control pulse, the duration of the "off" state can be adjusted [Fig. 4(c)].

In summary, we have realized an all-optically controlled THz polaritonic switch at room temperature based on the optical manipulation of polariton condensates in a 1D ZnO whispering gallery microcavity. A switching time of few hundreds of femtoseconds can be reached by parametric scattering of the polariton condensate by a time-delayed control pulse at different wavelengths. The off-state duration can be precisely tuned by the control power, and an extinction ratio of over 60 dB can be achieved. After the polariton population is switched off, a revival of the polariton population occurs at the picosecond timescale, which we attribute to the presence of remnant excitons which can again condense. We were able to explain quantitatively the effect by a parametric scattering model, where the polariton population is depleted due to a bosonically enhanced nonlinear two-photon process to the control mode. Such a two-photon process was confirmed to exist in the reverse direction.

To our knowledge, the ultrafast operation time and the high extinction ratios that we have achieved exhibit some of the most advanced characteristics for a room-temperature polariton-based switch. Compared to approaches based on gating by light-induced excitonic potentials [27,47], our switching speeds are about 100 times faster. Recent work reported an ultrafast polaritonic switch realized in an organic microcavity at room temperature [26] where a subpicosecond switching time and an extinction ratio of about 50 were achieved. Compared to this, our scheme can realize an all-optically controlled femtosecond polaritonic switching with a much higher extinction ratio of over 60 dB. We expect that our reported values are not at the fundamental limit, since the hybrid nature of polaritons provides a novel route for the manipulation of polariton dynamics at a much shorter timescale, based on the photonic part of polaritons. Our technique gives promise for high-speed polaritonic operating devices working in the strong-coupling regime at room temperature. Combined with the superfluid characteristics of polaritons with low-power dissipation, the mechanism reported in this work can be extended to other microcavity systems which could help to overcome the speed limits of polariton-based digital communication devices.

We thank Jingyan Feng for discussions. This work is supported by the National Key R&D Program of China (Grants No. 2018YFA0306303, No. 2018YFA0306304, No. 2021YFA1200803); the National Natural Science Foundation of China (Grants No. 92050105, No. 91950 201, No. 11674069, No. 11834004, No. 12174111, and No. 11574205); the Project supported by the Science and Technology Commission of Shanghai Municipality, China (Grants No. 22ZR1419700, No. 19ZR1473900). Z. C. acknowledges the support from the Fundamental Research Funds for the Central Universities (207202 00074) and the Interdisciplinary program of Wuhan National High Magnetic Field Center (Grant No. WHMFC202111). T. B. is supported by the National Natural Science Foundation of China (62071301); NYU-ECNU Institute of Physics at NYU Shanghai; the Joint Physics Research Institute Challenge Grant; the Science and Technology Commission of Shanghai Municipality (19XD1423000, 22ZR1444600); the NYU Shanghai Boost Fund; the China Foreign Experts Program (G2021013002L); the NYU Shanghai Major-Grants Seed Fund. Z. S. acknowledges the support from the Shanghai Pujiang Program Grant No. 21PJ1403000, and Joint Physics Research Institute Challenge Grant of the NYU-ECNU Institute of Physics at NYU Shanghai. F. C. acknowledges the support from the Fundamental Research Funds for the Central Universities (YBNLTS2022-007).

*hli@lps.ecnu.edu.cn
†tim.byrnes@nyu.edu
‡zhanghai@xmu.edu.cn
§jwu@phy.ecnu.edu.cn

[1] G. Jose and M. Ferreira, *Advances in Optoelectronic Technology and Industry Development: Proceedings of the 12th International Symposium on Photonics and Optoelectronics* (CRC Press, Xi'an, 2019).
[2] D. Dragoman and M. Dragoman, *Advanced Optoelectronic Devices* (Springer, Berlin Heidelberg, 2013).
[3] M. Kauranen and A. V. Zayats, Nat. Photonics **6**, 737 (2012).
[4] C. Li, *Nonlinear Optics: Principles and Applications* (Springer, Singapore, 2016).
[5] T. Volz, A. Reinhard, M. Winger, A. Badolato, K. J. Hennessy, E. L. Hu, and A. Imamoglu, Nat. Photonics **6**, 605 (2012).
[6] X. Y. Hu, P. Jiang, C. Y. Ding, H. Yang, and Q. H. Gong, Nat. Photonics **2**, 185 (2008).
[7] A. Schiffrin, T. Paasch-Colberg, N. Karpowicz, V. Apalkov, D. Gerster, S. Muhlbrandt, M. Korbman, J. Reichert, M. Schultze, S. Holzner, J. V. Barth, R. Kienberger, R. Ernstorfer, V. S. Yakovlev, M. I. Stockman, and F. Krausz, Nature (London) **493**, 70 (2013).
[8] A. Kavokin and G. Malpuech, *Cavity Polaritons* (Elsevier Science, Amsterdam, 2003).
[9] J. J. Hopfield, Phys. Rev. **112**, 1555 (1958).
[10] J. Kasprzak, M. Richard, S. Kundermann, A. Baas, P. Jeambrun, J. M. J. Keeling, F. M. Marchetti, M. H. Szymanska, R. Andre, J. L. Staehli, V. Savona, P. B. Littlewood, B. Deveaud, and L. S. Dang, Nature (London) **443**, 409 (2006).
[11] R. Balili, V. Hartwell, D. Snoke, L. Pfeiffer, and K. West, Science **316**, 1007–1010 (2007).
[12] M. H. Anderson, J. R. Ensher, M. R. Matthews, C. E. Wieman, and E. A. Cornell, Science **269**, 198 (1995).
[13] A. Amo, D. Sanvitto, F. P. Laussy, D. Ballarini, E. del Valle, M. D. Martin, A. Lemaitre, J. Bloch, D. N. Krizhanovskii, M. S. Skolnick, C. Tejedor, and L. Vina, Nature (London) **457**, 291 (2009).
[14] K. G. Lagoudakis, M. Wouters, M. Richard, A. Baas, I. Carusotto, R. Andre, L. Dang, and B. Deveaud-Pledran, Nat. Phys. **4**, 706 (2008).
[15] A. Amo, S. Pigeon, D. Sanvitto, V. G. Sala, R. Hivet, I. Carusotto, F. Pisanello, G. Lemenager, R. Houdre, E. Giacobino, C. Ciuti, and A. Bramati, Science **332**, 1167 (2011).
[16] M. Sich, D. N. Krizhanovskii, M. S. Skolnick, A. V. Gorbach, R. Hartley, D. V. Skryabin, E. A. Cerda-Mendez, K. Biermann, R. Hey, and P. V. Santos, Nat. Photonics **6**, 50 (2012).
[17] D. Sanvitto and S. Kena-Cohen, Nat. Mater. **15**, 1061 (2016).
[18] T. Horikiri, M. Yamaguchi, K. Kamide, Y. Matsuo, T. Byrnes, N. Ishida, A. Loffler, S. Hofling, Y. Shikano, T. Ogawa, A. Forchel, and Y. Yamamoto, Sci. Rep. **6**, 25655 (2016).
[19] L. Sun, S. Sun, H. Dong, W. Xie, M. Richard, L. Zhou, L. S. Dang, X. Shen, and Z. Chen, arXiv:1007.4686.
[20] S. Christopoulos, G. Baldassarri Hoger von Hogersthal, A. J. D. Grundy, P. G. Lagoudakis, A. V. Kavokin, J. J. Baumberg, G. Christmann, R. Butte, E. Feltin, J. F. Carlin, and N. Grandjean, Phys. Rev. Lett. **98**, 126405 (2007).
[21] R. Su, A. Fieramosca, Q. Zhang, H. S. Nguyen, E. Deleporte, Z. H. Chen, D. Sanvitto, T. C. H. Liew, and Q. H. Xiong, Nat. Mater. **20**, 1315 (2021).
[22] C. Ciuti, V. Savona, C. Piermarocchi, A. Quattropani, and P. Schwendimann, Phys. Rev. B **58**, 7926 (1998).
[23] S. I. Tsintzos, N. T. Pelekanos, G. Konstantinidis, Z. Hatzopoulos, and P. G. Savvidis, Nature (London) **453**, 372 (2008).
[24] S. Kena-Cohen and S. R. Forrest, Nat. Photonics **4**, 371 (2010).
[25] D. Ballarini, M. De Giorgi, E. Cancellieri, R. Houdre, E. Giacobino, R. Cingolani, A. Bramati, G. Gigli, and D. Sanvitto, Nat. Commun. **4**, 1778 (2013).
[26] A. V. Zasedatelev, A. V. Baranikov, D. Urbonas, F. Scafirimuto, U. Scherf, T. Stoferle, R. F. Mahrt, and P. G. Lagoudakis, Nat. Photonics **13**, 378 (2019).
[27] C. Anton, T. C. H. Liew, G. Tosi, M. D. Martin, T. Gao, Z. Hatzopoulos, P. S. Eldridge, P. G. Savvidis, and L. Vina, Appl. Phys. Lett. **101**, 261116 (2012).
[28] J. G. Feng, J. Wang, A. Fieramosca, R. Q. Bao, J. X. Zhao, R. Su, Y. T. Peng, T. C. H. Liew, D. Sanvitto, and Q. H. Xiong, Sci. Adv. **7**, eabj6627 (2021).

[29] A. Dreismann, H. Ohadi, Y. Redondo, R. Balili, Y. G. Rubo, S. I. Tsintzos, G. Deligeorgis, Z. Hatzopoulos, P. G. Savvidis, and J. J. Baumberg, Nat. Mater. **15**, 1074 (2016).
[30] A. V. Zasedatelev, A. V. Baranikov, D. Sannikov, D. Urbonas, F. Scafirimuto, V. Y. Shishkov, E. S. Andrianov, Y. E. Lozovik, U. Scherf, T. Stoferle, R. F. Mahrt, and P. G. Lagoudakis, Nature (London) **597**, 493 (2021).
[31] F. Chen, H Zhou, H. Li, J. H. Cao, S. Luo, Z. Sun, Z. Zhang, Z. Q. Shao, F. H. Sun, B. E. Zhou, H. X. Dong, H. L. Xu, H. X. Xu, A. Kavokin, Z. H. Chen, and J. Wu, Nano Lett. **22**, 2023 (2022).
[32] F. Chen, H. Li, H. Zhou, Z. Y. Ye, S. Luo, Z. Sun, F. H. Sun, J. W. Wang, H. L. Xu, H. X. Xu, Z. H. Chen, and J. Wu, J. Phys. Condens. Matter **34**, 024001 (2022).
[33] Z. Y. Ye, F. Chen, H. Zhou, S. Luo, F. H. Sun, Z. Sun, Y. L. Zheng, X. F. Chen, H. L. Xu, Z. H. Chen, H. Li, and J. Wu, J. Phys. Condens. Matter **34**, 22LT01 (2022).
[34] C. Ciuti, Phys. Rev. B **69**, 245304 (2004).
[35] G. Dasbach, C. Diederichs, J. Tignon, C. Ciuti, P. Roussignol, C. Delalande, M. Bayer, and A. Forchel, Phys. Rev. B **71**, 161308(R) (2005).
[36] L. Sun, Z. Chen, Q. Ren, K. Yu, L. Bai, W. Zhou, H. Xiong, Z. Q. Zhu, and X. Shen, Phys. Rev. Lett. **100**, 156403 (2008).
[37] A. Trichet, L. Sun, G. Pavlovic, N. A. Gippius, G. Malpuech, W. Xie, Z. Chen, M. Richard, and L. S. Dang, Phys. Rev. B **83**, 041302(R) (2011).
[38] J. R. Chen, T. C. Lu, Y. C. Wu, S. C. Lin, W. R. Liu, W. F. Hsieh, C. C. Kuo, and C. C. Lee, Appl. Phys. Lett. **94**, 061103 (2009).
[39] W. H. Liu, D. Xu, W. Xie, H. X. Dong, J. Lu, S. F. Zhang, X. C. Shen, and Z. H. Chen, Appl. Phys. Express **6**, 091101 (2013).
[40] See Supplemental Material at http://link.aps.org/supplemental/10.1103/PhysRevLett.129.057402, which includes Refs. [31,41–44].
[41] I. Musa, N. Qamhieh, and S. T. Mahmoud, Results Phys. **7**, 3552 (2017).
[42] L. Wang, D. Zhao, Z. Su, and D. Shen, Nanoscale Res. Lett. **7**, 106 (2012).
[43] M. Wouters and I. Carusotto, Phys. Rev. Lett. **99**, 140402 (2007).
[44] T. Byrnes, T. Horikiri, N. Ishida, M. Fraser, and Y. Yamamoto, Phys. Rev. B **85**, 075130 (2012).
[45] W. Xie, H. X. Dong, S. F. Zhang, L. X. Sun, W. H. Zhou, Y. J. Ling, J. Lu, X. C. Shen, and Z. H. Chen, Phys. Rev. Lett. **108**, 166401 (2012).
[46] S. Kundermann, M. Saba, C. Ciuti, T. Guillet, U. Oesterle, J. L. Staehli, and B. Deveaud, Phys. Rev. Lett. **91**, 107402 (2003).
[47] C. Anton, T. C. H. Liew, D. Sarkar, M. D. Martin, Z. Hatzopoulos, P. S. Eldridge, P. G. Savvidis, and L. Vina, Phys. Rev. B **89**, 235312 (2014).